

# Crystal field effects and the nature of the giant magnetostriction in terbium dititanate

I. V. Aleksandrov, B. V. Lidskiĭ, L. G. Mamsurova, M. G. Neĭgauz, K. S. Pigal'skiĭ, K. K. Pukhov, N. G. Trusevich, and L. G. Shcherbakova

*Institute of Chemical Physics, Academy of Sciences of the USSR*

(Submitted 24 June 1985)

Zh. Eksp. Teor. Fiz. **89**, 2230–2247 (December 1985)

An experimental study is made of the temperature and field dependences of the magnetostriction and magnetization, and also of the temperature dependences of the magnetic susceptibility, specific heat, and unit cell parameter for polycrystalline and single-crystal  $\text{Tb}_2\text{Ti}_2\text{O}_7$  over a wide range of temperatures and fields. A conclusion is reached as to the structure of the energy levels of the  $\text{Tb}^{3+}$  ion in  $\text{Tb}_2\text{Ti}_2\text{O}_7$ . An explanation is given in the framework of crystal field theory for all the observed magnetic effects, including, in particular, the giant magnetostriction in  $\text{Tb}_2\text{Ti}_2\text{O}_7$ . It is shown that the enormous values of the magnetostriction of paramagnetic terbium dititanate are due to the peculiar features of the energy spectrum of the  $\text{Tb}^{3+}$  ion in the crystal lattice of  $\text{Tb}_2\text{Ti}_2\text{O}_7$ .

## I. INTRODUCTION

In the study of the giant magnetostriction of rare earth paramagnets in recent years, much attention has been devoted to elucidating the microscopic nature of the effect.<sup>1–4</sup> This problem is also the subject of the present paper, in which we study a wide variety of the magnetic properties of the compound  $\text{Tb}_2\text{Ti}_2\text{O}_7$ , which exhibits the largest magnetostriction of any of the rare earth titanates ( $\Delta l/l \sim 10^{-3}$  at  $T = 4.2$  K and  $H \approx 60$  kOe) in the paramagnetic state.<sup>3</sup>

Terbium dititanate,  $\text{Tb}_2\text{Ti}_2\text{O}_7$ , is a member of the homologous series of cubic compounds of the pyrochlore type with general formula  $\text{Ln}_2\text{Ti}_2\text{O}_7$ , where Ln is a rare earth element between Sm and Lu (space group  $Fd\bar{3}m = O_h^7$ ). As our measurements have shown,<sup>5</sup> the other isostructural compounds of this series that have been studied (with Ln = Sm, Dy, Ho, Yb, Tm) have magnetostrictions of the ordinary size for paramagnets:  $\Delta l/l \sim 10^{-5} - 10^{-6}$ . It was therefore of interest to investigate the causes of the anomalously high values of  $\Delta l/l$  observed in terbium dititanate.

Magnetostriction arises in a paramagnet as a result of the interaction of the magnetic moments of the localized electrons with an external magnetic field; this interaction leads to a shift of the minimum of the electronic term, i.e., to displacements of the equilibrium positions of the nuclei of the local environment of each paramagnetic center, which alter ultimately the linear dimensions of the sample. Estimates<sup>3</sup> have shown that the crystal field model gives a satisfactory explanation of the magnitude and temperature dependence of the giant magnetostriction of terbium dititanate if it is assumed that the ions of this material have a low-lying electronic excited state (separated from the ground state by an amount  $\Delta \approx 15 - 20$  K).

For a detailed comparison of the crystal field model with the experimental data on the magnetostriction, we need to know the position of the electronic energy levels and the corresponding wave functions. However, the literature contains no direct spectroscopic data on the crystal field param-

eters in  $\text{Tb}_2\text{Ti}_2\text{O}_7$ . Furthermore, it is not always permissible to directly carry over to magnetically concentrated compounds the data obtained by optical spectroscopy and ESR for dilute compounds because the electric field of the crystal can change substantially on dilution.<sup>6</sup> In fact, as we show below, the crystalline field around a  $\text{Tb}^{3+}$  ion in the diluted compound  $\text{Tb}_{0.1}\text{Y}_{1.9}\text{Ti}_2\text{O}_7$  differs appreciably from the field in  $\text{Tb}_2\text{Ti}_2\text{O}_7$ .

The absence of spectroscopic data on the energy spectrum of the  $\text{Tb}^{3+}$  ion in  $\text{Tb}_2\text{Ti}_2\text{O}_7$  made it necessary for us to undertake an exhaustive study, including measurements of the temperature and field dependences of the magnetostriction, measurement of the temperature dependence of the susceptibility over a wide range of temperatures (1.7–300 K), measurement of the field and temperature dependences of the magnetization (1.7–10 K, in fields to 60 kOe) in both polycrystalline and single-crystal samples, measurement of the temperature dependence of the specific heat (1.7–20 K) and unit-cell parameter (4.2–300 K), and measurement of the elastic modulus at  $T = 300$  K on polycrystalline samples. The mathematical processing and theoretical analysis of the results in the framework of the static and dynamic crystal field theory have permitted us to draw conclusions about the system of energy levels of the paramagnetic ion  $\text{Tb}^{3+}$  in the crystalline field of the lattice and to give not only a qualitative but also a quantitative explanation of all the observed magnetic effects in  $\text{Tb}_2\text{Ti}_2\text{O}_7$ , including, in particular, the giant magnetostriction.

## II. EXPERIMENTAL TECHNIQUES

The magnetic properties were studied on single-crystal and polycrystalline samples. The  $\text{Tb}_2\text{Ti}_2\text{O}_7$  single crystal was grown by the Verneuil method, and the polycrystalline samples were prepared by both ordinary ceramic technology and the method of chemical coprecipitation.<sup>7</sup> The original materials were "especially pure"  $\text{TiCl}_4$  and  $\text{TiO}_2$  and 99.997% pure  $\text{Tb}_4\text{O}_7$ . The phase composition was moni-

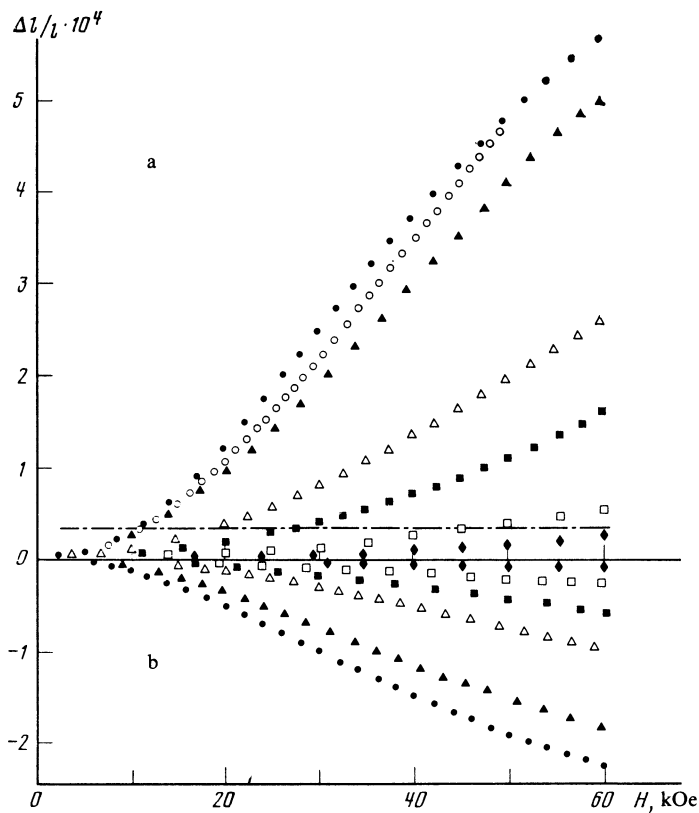


FIG. 1. Magnetic-field dependence of the magnetostriction of  $\text{Tb}_2\text{Ti}_2\text{O}_7$  for measurements parallel (a) and perpendicular (b) to the field. For a polycrystalline sample at temperatures  $T$  [K]: ● 4.2; ▲ 8; △ 16; ■ 25; □ 50; ◆ 78. For a single crystal: ○ along the [111] direction at 4.2 K. The dash-dot line is the magnetostriction of electrolytic nickel.

tored by x-ray diffraction on a DRON-2 diffractometer.

The susceptibility and magnetization of the polycrystalline and single-crystals samples along the [100] direction were measured by the Faraday balance method on an Oxford Instruments apparatus. The error in the measurement did not exceed 1.5% over the entire range of temperatures and fields. The measurements were made on cylindrical samples so that the demagnetizing factor could be more accurately taken into account.

The magnetization of the single crystal along the principal crystallographic directions [100], [110], and [111] was measured on a vibration magnetometer.<sup>8</sup> The error in the orientation of the samples (by x-ray diffraction) was less than 3°.

The magnetostriction measurements were made by a bridge method with a resistance strain gauge made of an alloy having a small galvanomagnetic effect. The samples were placed in a helium cryostat equipped with a superconducting solenoid and a system of vacuum jackets which permitted measurements in the temperature range 4.2–300 K.

The specific heat of the polycrystalline  $\text{Tb}_2\text{Ti}_2\text{O}_7$  was measured with a low-temperature adiabatic calorimeter to an accuracy of 3% by the method of pulsed heating.

The temperature dependence of the lattice parameter was obtained on a Geigerflex diffractometer equipped with a flow-through cryostat which permitted temperature stabilization to within 0.1 K. The lattice parameter was determined to an accuracy of  $\pm 0.0005 \text{ \AA}$  using the (880) reflection,  $2\theta = 120^\circ$ .

An estimate of the elastic constant was obtained from measurements of the velocity of a longitudinal ultrasonic

wave propagating in a polycrystalline sample of  $\text{Tb}_2\text{Ti}_2\text{O}_7$ .

### III. EXPERIMENTAL RESULTS AND DISCUSSION

Figure 1 shows the results of measurements of the field dependence of the magnetostriction of a polycrystalline sample of  $\text{Tb}_2\text{Ti}_2\text{O}_7$  in the temperature range 4.7–80 K and in a single crystal of  $\text{Tb}_2\text{Ti}_2\text{O}_7$  at  $T = 4.2 \text{ K}$ . The measurements were made both along the magnetic field,  $(\Delta l/l)_\parallel$ , and in the direction perpendicular to the field,  $(\Delta l/l)_\perp$ . It is seen that  $(\Delta l/l)_\parallel$  decreases as the temperature is raised, but it remains rather large, and only at liquid-nitrogen temperature does it reach values corresponding to  $\Delta l/l$  for ferromagnetic nickel. It turned out that  $(\Delta l/l)_\perp$  is opposite in sign to  $(\Delta l/l)_\parallel$ , and the experimental values of these quantities obey the inequality

$$\frac{1}{3}[(\Delta l/l)_\parallel + 2(\Delta l/l)_\perp] \ll (\Delta l/l)_\parallel. \quad (1)$$

We note that the expression in the square brackets characterizes the volume magnetostriction  $\Delta V/V$ ; our result thus shows that the linear striction is predominant in this compound.

As is seen in Fig. 1, the magnetostriction measured along the [111] direction in the single-crystal sample, though somewhat smaller in magnitude, is very similar in behavior to the magnetostriction of the polycrystalline material.

Figure 2a shows the temperature dependence of the inverse susceptibility  $\chi^{-1}$  of  $\text{Tb}_2\text{Ti}_2\text{O}_7$  in the temperature range 1.7–300 K for polycrystalline samples and for a single crystal (in the [100] and [111] directions); the measure-

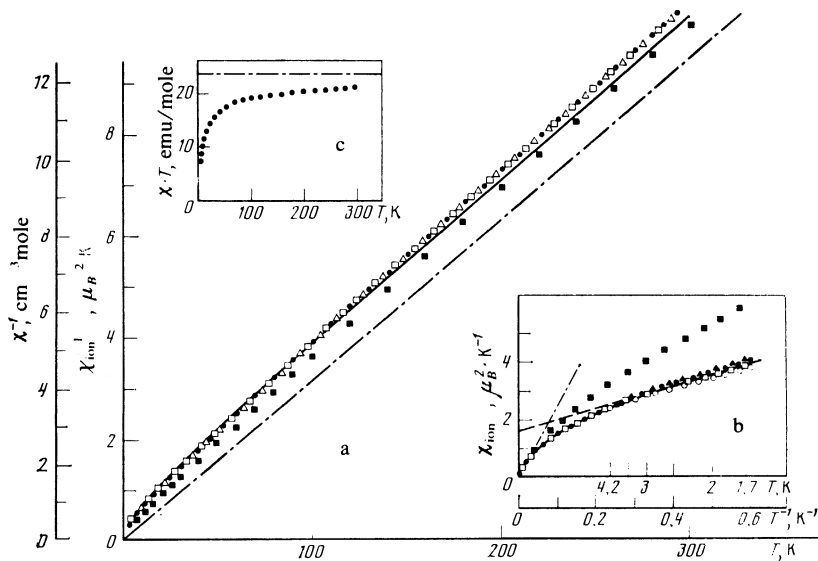


FIG. 2. Inverse susceptibility  $\chi^{-1}$  versus the temperature (a), the susceptibility versus  $T^{-1}$  (b), and  $\chi T$  versus the temperature (c). The points are experimental:  $\square, \Delta$ )  $\text{Tb}_2\text{Ti}_2\text{O}_7$  single crystal along the [100] and [111] directions, respectively;  $\bullet, \circ, \blacktriangle$ ) polycrystalline samples of  $\text{Tb}_2\text{Ti}_2\text{O}_7$  prepared in different lots;  $\blacksquare$ ) polycrystalline  $\text{Tb}_{0.1}\text{Y}_{1.9}\text{Ti}_2\text{O}_7$ . The solid curves are calculated according to the version-I level system (see Table I). The dot-dash lines in parts a and c are for the free  $\text{Tb}^{3+}$  ion, that in part b is for the doublet  $|\pm 6\rangle$ .

ments were made in a field of 0.5 kOe. The results for the two kinds of sample agree, as would be expected for a cubic compound. We see that the sample remains in the paramagnetic state all the way to 1.7 K, but the Curie-Weiss law is not obeyed: for  $T < 100$  K there is a deviation from straight-line behavior that is most pronounced below 20 K.

The overall form of  $\chi^{-1}(T)$  permits the assumption that in the temperature range under study the thermal energy  $kT$  is comparable to the values of the Stark splittings of the sublevels of the ground-state multiplet, and as the temperature is raised to 300 K a successive occupation of the series of energy levels occurs. However, as we see from the plot of  $\chi T$  versus temperature in Fig. 2c, nowhere near all of the sublevels of the ground state  ${}^7F_6$  of the trivalent terbium ion are occupied.

We see from Fig. 2b that the ground state does not cor-

respond to the maximum projection of the angular momentum  $J_z = \pm 6$  observed for a number of terbium compounds in which the symmetry of the crystalline fields is lower than axial.<sup>9</sup> In fact, in the region of the lowest temperatures, where it can be assumed with a high probability that only the lowest doublet is occupied,  $\chi(1/T)$  (the dashed line in Fig. 2b) is of the form

$$\chi = C/T + \alpha, \quad (2)$$

where  $C = 2.8 \text{ cm}^3 \text{ deg/mole}$  and  $\alpha = 1.3 \text{ cm}^3/\text{mole}$ . Because  $C = 2Ng_j^2\mu_B^2 \langle \hat{J}_z \rangle^2 / 3k$  for a doublet, we can determine the average value of the z component of the angular momentum:  $\langle \hat{J}_z \rangle = 2.23 \pm 0.15$ . (Here the coefficient 1/3 arises in the averaging over angles for the polycrystalline material or over nonequivalent  $\text{Tb}^{3+}$  sites for the single crystal,  $N$  is Avogadro's number,  $g_j$  is the Landé factor ( $g_j = 3/2$  for

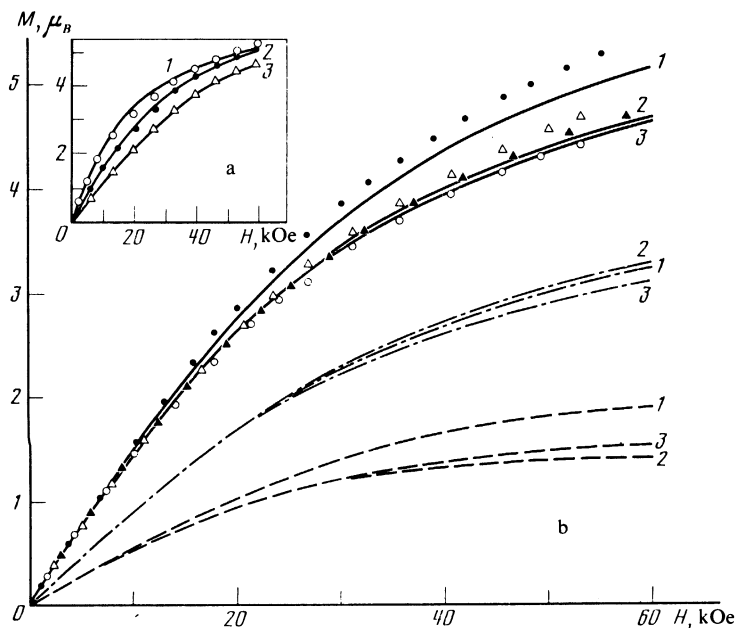


FIG. 3. a) Magnetic moment of polycrystalline  $\text{Tb}_2\text{Ti}_2\text{O}_7$  versus the external magnetic field at various temperatures:  $\circ, 1$ ) 1.7 K;  $\bullet, 2$ ) 4.3 K;  $\Delta, 3$ ) 8 K. The points are experimental, the solid curves are calculated for the version-I level system. b) Magnetic moment of a  $\text{Tb}_2\text{Ti}_2\text{O}_7$  single crystal versus the magnetic field at  $T = 4.8$  K along different crystallographic directions:  $\bullet, 1$ ) [100];  $\Delta, 2$ ) [110];  $\circ, 3$ ) [111]. The points are experimental [ $\blacktriangle$  is  $M(H)$  for polycrystalline  $\text{Tb}_2\text{Ti}_2\text{O}_7$  at  $T = 4.8$  K]. The curves are calculated: the solid curves for the version-I level system along the same directions; the dashed curves for the ground state of the  $\text{Tb}^{3+}$  ion with  $\mu = 2.35g_j\mu_B$ ; the dot-dash curve is the difference between the experimental  $M(H)$  curve and the  $M(H)$  curve corresponding to the ground state.

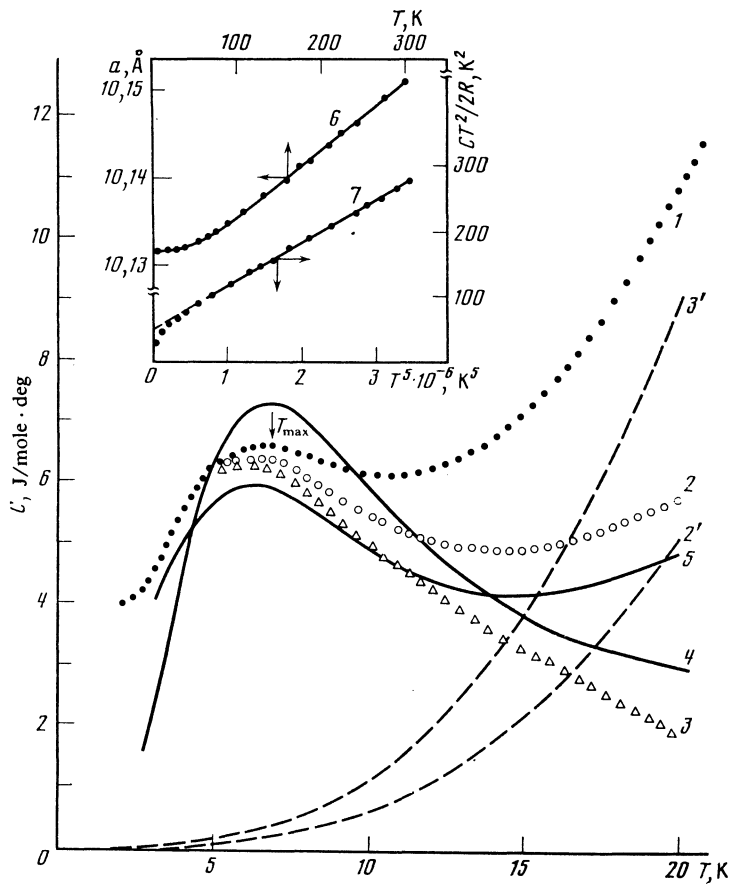


FIG. 4. Temperature dependence of the specific heat of  $\text{Tb}_2\text{Ti}_2\text{O}_7$ : 1) experimental points; 2', 3') the specific heat of the lattice for  $\Theta_D = 320$  and  $266$  K, respectively; 2, 3) the curves obtained after subtraction of the experimental dependence of the corresponding lattice contributions 2' and 3'; 4, 5) calculated curves for versions I and II, respectively. Inset: 6) temperature dependence of the unit-cell parameter of  $\text{Tb}_2\text{Ti}_2\text{O}_7$  (the points are experimental, the solid curve is calculated); 7)  $CT^2/2R$  versus  $T^5$ .

$\text{Tb}^{3+}$ ),  $\mu_B$  is the Bohr magneton, and  $k$  is the Boltzmann constant.)

It should be noted that our estimates of  $C$  and  $\alpha$  did not take into account the contribution from the interaction between the paramagnetic ions, which is rather small and can lead to magnetic ordering only for  $T \lesssim 1$  K. This interaction cannot be taken into account with the aid of measurements on the dilute ( $\text{Tb}_{0.1}\text{Y}_{1.9}\text{Ti}_2\text{O}_7$ ) sample. As we see from Fig. 2a, the  $\chi^{-1}(T)$  curve for this sample does not correspond to a parallel shift of the curve for the concentrated compound, indicating that the crystalline field around the  $\text{Tb}^{3+}$  ions changes upon the substitution of  $\text{Y}^{3+}$ .

The rather large value of  $\alpha$  given above indicates that the ground state contains a strong admixture of the excited states. This effect, which can be attributed to the proximity of these states, is also suggested by the magnetization isotherms shown in Fig. 3a. The  $M(H)$  curves do not exhibit saturation even at  $T = 1.7$  K and in strong magnetic fields  $\approx 60$  kOe. Measurements on the single-crystal sample along different crystallographic directions revealed a small anisotropy of the magnetic moment in  $\text{Tb}_2\text{Ti}_2\text{O}_7$ , with the "easy" direction being  $[100]$  (Fig. 3b).

The most direct indication of the presence of energy levels lying close to the ground state can be obtained from the temperature dependence of the specific heat. Figure 4 shows the measured temperature dependence  $C(T)$  for polycrystalline  $\text{Tb}_2\text{Ti}_2\text{O}_7$  (curve 1). We see that the experimental curve has a gentle anomaly near  $T \approx 7$  K, implying that

curve 1 is the sum of at least two components: an anomaly of the Schottky type, corresponding to the population of the nearby excited state, and the lattice specific heat.

The lattice specific heat was determined in two ways: from measurements of the isostructural diamagnetic dititanate  $\text{Y}_2\text{Ti}_2\text{O}_7$  and by constructing the curve of  $CT^2(T^5)$  for  $T > T_{\text{max}}$ .

It turned out that in addition to the main contribution that is proportional to  $BT^3$ , the specific heat of  $\text{Y}_2\text{Ti}_2\text{O}_7$  contains a small contribution which is approximately linear in temperature. For this reason there is a large error in the determination of the coefficient  $B$  and the corresponding value of the Debye temperature for  $\text{Y}_2\text{Ti}_2\text{O}_7$ :  $\Theta_D = 470 \pm 70$  K.

Using the empirical relation  $\Theta_D \propto (\bar{M}_0 \bar{V}_0)^{-1/2}$ , where  $\bar{M}_0$  is the average atomic mass and  $\bar{V}_0$  is the average volume occupied by one atom in the sample, we obtain for  $\text{Tb}_2\text{Ti}_2\text{O}_7$  the estimate  $\Theta_D = 320 \pm 50$  K. The lattice specific heat corresponding to  $\Theta_D = 320$  K is given by curve 2' in Fig. 4.

Curve 7 in the inset in Fig. 4 illustrates the second method of determining the lattice specific heat of  $\text{Tb}_2\text{Ti}_2\text{O}_7$ . We see that in the temperature range 15–20 K the experimental specific heat is described well by the function

$$C/2R = a/T^2 + bT^3 \quad (3)$$

with coefficients  $a = 49.3 \text{ K}^2$  and  $b = 6.86 \cdot 10^{-5} \text{ K}^{-3}$  ( $R$  is the universal gas constant). Here the first term represents the "tail" of the Schottky-type anomaly, and the second

term corresponds to the lattice specific heat. The value of the coefficient  $b$  gives an estimate of  $\Theta_D = 266$  K for the Debye temperature; the corresponding lattice contribution is shown by curve 3' in Fig. 4.

Thus, as a result of the difference in the values of  $\Theta_D$  estimated by different methods, uncertainty arises in the value and behavior for  $T < 10$  K of the part of the specific heat (curves 2 and 3 in Fig. 4) that remains after subtraction of the lattice contribution from the experimental  $C(T)$  curve. While curve 3 corresponds to a large degree to a simple Schottky anomaly for a two-level system, curve 2 corresponds to the successive occupation of a whole series of excited states. The  $C(T)$  curves calculated for these two versions by the Schottky formula

$$C = \left[ \omega_0 \sum_{i=1}^n \omega_i E_i^2 \exp\left(-\frac{E_i}{T}\right) + \sum_{i>j} \omega_i \omega_j (E_i - E_j)^2 \exp\left(-\frac{(E_i + E_j)}{T}\right) \right] \times T^{-2} \left[ \omega_0 + \sum_{i=1}^n \omega_i \exp\left(-\frac{E_i}{T}\right) \right]^{-2}, \quad (4)$$

are given by curves 4 and 5 in Fig. 4 ( $\omega_0$  and  $\omega_i$  are the multiplicity of the ground state and  $i$ th state, respectively, and  $E_i$  is the energy of the  $i$ th level).

In the first case the level system consists of two doublets split by a gap  $\Delta = 16$  K (curve 4), and the next excited levels are found at 70 K or higher. In the second case the nearest singlet is separated from the ground doublet by a distance  $\Delta_1 = 10$  K, the next singlet by a distance  $\Delta_2 = 21$  K, and two more levels (a singlet and a doublet) are separated from the ground state by  $\Delta_3, \Delta_4 \approx 90-100$  K.

It should be noted that in order to bring the initial parts of the experimental and theoretical  $C(T)$  curves into agreement for  $T < 4$  K, we would have to assume that the ground doublet is split by  $\approx 1$  K, as could occur for various reasons, including a small exchange interaction or the presence of structural defects in the compound under study.<sup>11</sup> If the latter reason is correct, this would also explain the disagreement between the experimental and theoretical values of the specific heat in the region of the maximum. For example, better agreement of curves 4 and 3 can be obtained by introducing a Gaussian distribution for the splitting of the energy levels (for an average splitting  $\Delta \approx 16$  K the half-width can amount to  $\delta_T \approx 3$  K). Thus, solely on the basis of the behavior of the specific heat in the temperature region under study, one cannot decide in favor of one of the two versions indicated above.

Additional information on the value of  $\Theta_D$  can be obtained by studying the temperature dependence of the coefficient of thermal expansion (although it should be noted that the Debye temperature determined by this method does not necessarily coincide strictly with the specific-heat data). Curve 6 in the inset in Fig. 4 shows the measured temperature dependence of the unit-cell parameter in the region 4.2–300 K. We see that as the temperature is lowered from room temperature to 100 K the  $a(T)$  curve is linear, indicating

that in this temperature range the coefficient of thermal expansion is constant and equal to  $\alpha = 8.2 \cdot 10^{-6} \text{ deg}^{-1}$ . The  $a(T)$  curve can be described in its entirety by the equation

$$a(T) = a(0) + ATF(T/\Theta_D), \quad (5)$$

which is obtained by the Grüneisen relation between the coefficient of linear expansion and the specific heat  $C_V$ . Here

$$F(T/\Theta_D) = \frac{1}{T} \int_0^T C_V dT$$

is a tabulated function given for each value of the ratio  $T/\Theta_D$ . The constant  $A$  is determined from any two values  $a_1$  and  $a_2$  of the lattice parameter at temperatures  $T_1$  and  $T_2$ , respectively. By adjusting the parameter  $T/\Theta_D$  to give the best agreement of the theoretical and experimental  $a(T)$  curves over the entire temperature range of the measurements, we obtain an estimate for  $\Theta_D$  that lies in the range 180–240 K. Solid curve 6 in the inset in Fig. 4 is the  $a(T)$  curve calculated according to (5) for  $\Theta_D = 200$  K. Our estimate  $180 < \Theta_D < 240$  K agrees better with the value of the Debye temperature that corresponds to the second method of determining the lattice contribution to the specific heat. Evidently, the value of  $\Theta_D$  obtained from the measurements of the specific heat on a diamagnetic sample is insufficiently accurate in the present case as a result of the large difference in the molecular weights of  $\text{Y}_2\text{Ti}_2\text{O}_7$  and  $\text{Tb}_2\text{Ti}_2\text{O}_7$  and the inadmissibility of using the relation  $\Theta_D \propto (\bar{M}_0 \bar{V}_0)^{-1/2}$  to convert from the compound  $\text{Y}_2\text{Ti}_2\text{O}_7$  to the compound  $\text{Tb}_2\text{Ti}_2\text{O}_7$ . Thus the experimental temperature dependence of the specific heat agrees better with the version of a simple two-level system with  $\Delta = 16$  K.

In addition, in regard to the measurements of the temperature dependence  $a(T)$ , it should be noted that because the  $a(T)$  curve corresponds within the experimental error to the Debye form, because no broadening or bifurcation of the (880) peak is observed, and because the diffractometer traces correspond to a cubic structure of the pyrochlore type down to  $T = 4.2$  K, we can conclude that no structural distortions occur in the sample and that the cubic structure remains stable all the way down to liquid-helium temperature.

#### IV. DETERMINATION OF THE ENERGY LEVEL SYSTEM OF THE $\text{Tb}^{3+}$ ION

The unit cell of  $\text{Ln}_2\text{Ti}_2\text{O}_7$  (for  $\text{Tb}_2\text{Ti}_2\text{O}_7$   $a = 10.146$  Å) contains 8 formula units, i.e., 16  $\text{Ln}^{3+}$  ions in sites of trigonal symmetry  $D_{3d}$ . Each  $\text{Ln}^{3+}$  ion is surrounded by 8 oxygen ions, which form a distorted cube. Two diametrically opposed oxygen ions are located at the corners of this cube, and the remaining six ions are somewhat displaced from their ideal positions and are found near the equatorial plane perpendicular to the diagonal of the cube or to the trigonal axis (Fig. 5). The location of the last six oxygen ions is determined by the position parameter  $x$ , which for several investigated compounds of the  $\text{Ln}_2\text{Ti}_2\text{O}_7$  type ( $\text{Ln} = \text{Er}, \text{Y}$ ) is approximately 0.33.<sup>10</sup> However, no information on the parameter  $x$  for  $\text{Tb}_2\text{Ti}_2\text{O}_7$  is found in the literature.

The value  $x = 3/8$  corresponds to the case of a purely

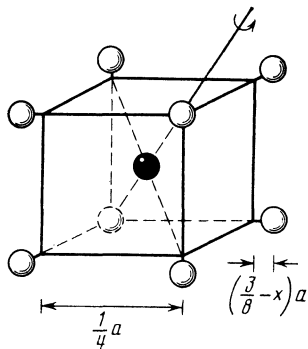


FIG. 5. Nearest-oxygen environment of the  $\text{Ln}^{3+}$  ion in a cubic structure of the pyrochlore type with formula  $\text{Ln}_2\text{Ti}_2\text{O}_7$ ;  $a$ ) unit-cell parameter;  $x$ ) position parameter of the oxygen ions; (●)  $\text{Ln}^{3+}$ , (○)  $\text{O}^{2-}$ .

cubic symmetry, when all the oxygen ions are located exactly at the corners of the cube. The value  $x = 2/8$  corresponds to the situation in which six  $\text{O}^{2-}$  ions are found in the equatorial plane perpendicular to the  $[111]$  axis, i.e., there is a sixfold axis and the environment of the terbium ion has hexagonal symmetry. For  $2/8 < x < 3/8$  there is a threefold inversion axis, and the case under study, with symmetry  $D_{3d}$ , can be regarded as intermediate between the two extreme cases discussed above.

In a crystalline field with symmetry  $D_{3d}$  the thirteen-fold degenerate ground state  ${}^7F_6$  of the  $\text{Tb}^{3+}$  ion is split into four doublets and five singlets according to the scheme

$${}^7F_6 \rightarrow 3\Gamma_1^T + 2\Gamma_2^T + 4\Gamma_3^T.$$

In the absence of an external magnetic field and in the absence of an interaction between the magnetic ions, the Hamiltonian of the  $\text{Tb}^{3+}$  ion in the general case depends on six parameters:

$$\mathcal{H}_{\text{cr}} = B_2^0 O_2^0 + B_4^0 O_4^0 + B_4^3 O_4^3 + B_6^0 O_6^0 + B_6^3 O_6^3 + B_6^6 O_6^6 \quad (6)$$

(the  $z$  axis is taken in the direction of the trigonal axis). By adjusting the parameters  $B_k^m$  of the crystalline field to give the best agreement between the theoretical curves and all the available experimental curves, we can determine the energy spectrum of the  $\text{Tb}^{3+}$  ion.

In view of the absence of initial data on the possible values of the parameters in compounds analogous to the compound under study and in view of the complexity of introducing some kind of parametrization that would enable us to narrow the region of variation of the six parameters, the problem was not solved in general form but with the following two approximations.

In the case of a small trigonal distortion of the local cubic symmetry, Hamiltonian (6) can be replaced by the Hamiltonian

$$\mathcal{H}_{\text{cr}} = \mathcal{H}_{\text{cub}} + B_2^0 O_2^0, \quad (7)$$

where

$$\mathcal{H}_{\text{cub}} = B_4^0 (O_4^0 + 2\sqrt{2} O_4^3) + B_6^0 \left( O_6^0 - \frac{35}{2\sqrt{2}} O_6^3 + \frac{77}{8} O_6^6 \right).$$

In the other limiting cases, where the position parameter is close to the value  $2/8$ , the terms  $B_4^3$  and  $B_6^3$  in Hamil-

tonian (6) can be set equal to zero, which actually corresponds to hexagonal symmetry.

When the Hamiltonian of the problem contains no more than four parameters, one can introduce a parametrization; it is convenient to choose as parameters the distances  $\Delta_1$  and  $\Delta_2$  between the lowest levels or the magnetic moments  $\mu_1$  and  $\mu_2$  of the ground-state doublet and first excited level, respectively, or a combination of these. The region of variation of the parameters  $\mu_1$ ,  $\Delta_1$ , and  $\Delta_2$  was set by analyzing the experimental curves of  $\chi(T)$ ,  $M(H, T)$ , and  $C(T)$  given above. The numerical processing of the data was done on a computer.

The magnetic susceptibility for the single-crystal and polycrystalline samples in the temperature range 1.7–300 K were calculated by the formula

$$\chi = \frac{g_J^2 \mu_B^2}{3kT} \left[ \sum_{n,\alpha} \rho_n |\langle n | \hat{J}_\alpha | n \rangle|^2 + \sum_{n \neq n', \alpha} \frac{\rho_{n'} - \rho_n}{(E_n - E_{n'})/T} |\langle n | \hat{J}_\alpha | n' \rangle|^2 \right], \quad (8)$$

$$\rho_n = \exp\left(-\frac{E_n}{T}\right) / \sum_{n'} \exp\left(-\frac{E_{n'}}{T}\right),$$

where  $\rho_n$  is the population of the  $n$ th level,  $E_n$  and  $|n\rangle$  are the eigenvalues and eigenfunctions of the operator  $\mathcal{H}_{\text{cr}}$ , and  $\hat{J}_\alpha$  ( $\alpha = x, y, z$ ) are the components of the total angular momentum  $\hat{\mathbf{J}}$ .

The magnetization was calculated on the basis of the Hamiltonian

$$\mathcal{H}_0 = \mathcal{H}_{\text{cr}} + \mathcal{H}_z = \mathcal{H}_{\text{cr}} + g_J \mu_B \mathbf{H} \hat{\mathbf{J}}, \quad (9)$$

where  $\mathbf{H}$  is the external magnetic field. For a polycrystalline sample the magnetization along the field  $\mathbf{H}$  (per  $\text{Tb}^{3+}$  ion) is given by the expression

$$M = \frac{1}{4\pi} \int_0^{2\pi} d\varphi \int_0^\pi M(\theta, \varphi) \sin \theta d\theta, \quad (10)$$

where

$$M(\theta, \varphi) = -g_J \mu_B \sum_n \frac{\rho_n}{H} \langle n | \hat{\mathbf{J}} \mathbf{H} | n \rangle.$$

In a single crystal having a cubic unit cell with 16  $\text{Tb}^{3+}$  ions in an environment whose local symmetry ( $D_{3d}$ ) is lower than cubic, there must exist no fewer than four nonequivalent sites for the  $\text{Tb}^{3+}$  ions, corresponding to the four space diagonals of the cube, which are codirectional with the trigonal axes along which the distortion occurs. The magnetization of the single crystal along the field is therefore given by the expression

$$M = \frac{1}{4} \sum_{i=1}^4 M(\theta_i, \varphi_i), \quad (11)$$

where  $\theta_i$  and  $\varphi_i$  are the polar and azimuthal angles of the field  $\mathbf{H}$  with respect to a coordinate system with the  $z$  axis chosen along the  $i$ th diagonal of the cubic unit cell. In each case where the field  $\mathbf{H}$  is directed along an axis of the type  $[100]$ ,  $[110]$ , or  $[111]$ , the angles  $\theta_i$  and  $\varphi_i$  are determined

TABLE I. System of energy levels of the  $Tb^{3+}$  ion in  $Tb_2Ti_2O_7$ .

Irreducible representation	Wave functions	Energy, K
$\Gamma_3^T$	$\psi_{1,2}=0.747 \pm 5\rangle-0.665 \mp 4\rangle$	0
$\Gamma_3^T$	$\psi_{3,4}=0.816 \pm 4\rangle-0.577 \mp 2\rangle$	16
$\Gamma_1^T$	$\psi_5=0.061 6\rangle-0.996 0\rangle+0.061 -6\rangle$	101
$\Gamma_2^T$	$\psi_6=0.707 -3\rangle-0.707 3\rangle$	114
$\Gamma_3^T$	$\psi_{7,8}=0.665 \pm 5\rangle+0.747 \mp 4\rangle$	343
$\Gamma_3^T$	$\psi_{9,10}=0.577 \pm 4\rangle+0.816 \mp 2\rangle$	503
$\Gamma_1^T$	$\psi_{11}=0.707 -3\rangle+0.707 3\rangle$	618
$\Gamma_2^T$	$\psi_{12}=0.707 6\rangle-0.707 -6\rangle$	1617
$\Gamma_1^T$	$\psi_{13}=0.705 6\rangle+0.085 0\rangle+0.705 -6\rangle$	1628

from simple geometrical considerations.

A calculation based on Hamiltonian (7) did not give satisfactory agreement of the theoretical and experimental curves. Evidently the distortion of the local cubic symmetry of the  $Tb^{3+}$  ions in  $Tb_2Ti_2O_7$  is actually large, and the parameter differs appreciably from the value  $3/8$ .

A processing of the data on the basis of Hamiltonian (6) with  $B_2^3 = 0$  and  $B_4^3 = 0$  showed that calculations based solely on an analysis of the curves of the susceptibility  $\chi(T)$  and magnetization  $M(T)$  for polycrystalline  $Tb_2Ti_2O_7$  give a set of solutions which agree with experiment to within 4–5%. The  $C(T)$  curve for the polycrystalline material and the  $M(H)$  curve for different directions in the single crystal in the high-field region turned out to be more sensitive to the system of energy levels, and served as the main criterion in our analysis of the different versions. For example, a processing of all the available data for the polycrystalline material, including the  $C(T)$  curve, allowed us to rule out the versions with a singlet ground state and to select from the remaining level systems only two versions for which there is satisfactory agreement of the theoretical and experimental curves:

Version I (doublet-doublet):

$$2.2g_J\mu_B < \mu_1 < 2.5g_J\mu_B,$$

$$1.8g_J\mu_B < \mu_2 < 3.8g_J\mu_B, \quad 14 \text{ K} < \Delta_1 < 16 \text{ K}, \quad \Delta_2 > 70 \text{ K}.$$

Version II (doublet-singlet-singlet):

$$2.2g_J\mu_B < \mu_1 < 2.6g_J\mu_B,$$

$$\mu_2 = 0, \quad \mu_3 = 0, \quad 7 \text{ K} < \Delta_1 < 14 \text{ K}, \quad 16 \text{ K} < \Delta_2 < 25 \text{ K}, \quad \Delta_3, \Delta_4 > 70 \text{ K}.$$

Figures 2–4 show the calculated curves of  $\chi(T)$ ,  $M(H, T)$ , and  $C(T)$  for the version-I level system with the parameters (in  $\text{cm}^{-1}$ ):

$$B_2^0 = -667 \langle J || \alpha || J \rangle, \quad B_4^0 = 373 \langle J || \beta || J \rangle, \quad (12)$$

$$B_6^0 = -530 \langle J || \gamma || J \rangle, \quad B_8^0 = -5175 \langle J || \gamma || J \rangle,$$

where  $\langle J || \alpha || J \rangle$ ,  $\langle J || \beta || J \rangle$ ,  $\langle J || \gamma || J \rangle$  are the reduced matrix elements.<sup>9</sup> The wave functions  $\psi_i$  and energies of the states are given in Table I. We see from Figs. 2–4 that the agreement of all the theoretical and experimental curves is good except for two parts of the specific heat curve, for  $1 < T < 4 \text{ K}$  and in the region of  $T_{\text{max}}$ ; these parts, as we mentioned in Sec. III above, can be brought into better agreement by taking into account the imperfection of the pyrochlore structure.

Figure 4 also shows the calculated  $C(T)$  curve (curve 5) corresponding to the second version of the level system; this curve agrees better with the experimental curve in the two regions indicated than does curve 4. For this version the ground level is a non-Kramers doublet  $0.894|\mp 4\rangle - 0.447|\pm 2\rangle$  with two nearby singlets  $0.695|-6\rangle - 0.181|0\rangle + 0.695|+6\rangle$  and  $0.707|-3\rangle - 0.707|+3\rangle$  at distances of  $\Delta_1 = 10 \text{ K}$  and  $\Delta_2 = 21 \text{ K}$ . Two more levels (a doublet and a singlet at distances  $\Delta_3 = 94 \text{ K}$  and  $\Delta_4 = 105 \text{ K}$ ) give a larger value of the “tail” of the specific heat than on the curve for version I. However, the version-II level system has the shortcoming that the  $M(H)$  curves calculated for different directions in the single crystal exhibit a very insignificant anisotropy compared to that observed in experiment. To ascertain whether this circumstance could be decisive in the final choice of level system, let us consider in more detail the nature of the magnetic anisotropy in the compound under study.

Figure 3b shows the calculated  $M(H)$  curves for the ground level—an isolated non-Kramers doublet ( $\psi_1, \psi_2$ ) with  $\mu_1 = 2.35\mu_B g_J$ —after averaging over the nonequivalent sites. These curves clearly demonstrate the role of the nonequivalence of the  $Tb^{3+}$  ions, which not only affects the absolute value of the anisotropy but also determines which of the directions will have the maximum magnetic moment. In fact, in a crystalline field of hexagonal symmetry the external-field induced magnetic moments of the  $Tb^{3+}$  ions are oriented along the directions of the trigonal axes, which coincide with the directions of the four space diagonals of the cubic unit cell. As a result of the summation over the four nonequivalent sites, the projections of the moments onto directions of the [100] and [110] types turn out to be such that the anisotropy amounts to 26% in absolute value (Fig. 3b), and the maximum moment is in the [100] direction.

The existence of an excited level at a distance  $\Delta \approx 16 \text{ K}$  causes the resultant magnetic moment to be larger by a factor of three than the moment of the ground state, but the value of the anisotropy is changed only insignificantly. The latter circumstance is also due to the nonequivalence of the  $Tb^{3+}$  ions. A simple calculation shows that if the condition  $\Delta \gg \mu_B H$ ,  $\Delta \gg kT$  were satisfied (so that the resultant magnetic moment could be regarded as the sum of two contributions: the magnetic moment of the ground state and the Van Vleck contribution), after the summation over the four nonequivalent sites the additional contribution due to the admixture of the excited states to the ground state would come out linear in  $H$  and isotropic. Consequently, the anisotropy

of the resultant moment would be the same as for the ground state.

The slight increase in the anisotropy of the resultant moment in comparison with the ground state and the different order of the [111] and [110] axes are due to the fact that in  $Tb_2Ti_2O_7$  the excited level lies quite low ( $\Delta_1 = 16$  K), and the additional contribution to the resultant moment is no longer linear and isotropic. Figure 3b shows the calculated curves representing the difference between the resultant moment of  $Tb_2Ti_2O_7$  and the moment of the isolated ground state for version I, i.e., the additional contribution due mainly to the presence of a nearby excited level.

An analogous calculation for the second version, in which there are two singlets at distances  $\Delta_1 = 10$  K and  $\Delta_2 = 21$  K, gives a result which differs from that discussed above. In fact, in this case the lower singlet is not mixed with the ground state by the magnetic field, and, being occupied at 4.8 K, causes a slight decrease in the magnetic moment of the ground state. The contribution to the anisotropy from the admixture of the second singlet is such that the resultant  $M(H)$  curve exhibits practically no anisotropy.

It turns out that this result, which was obtained for a specific version II, is valid for any other doublet-singlet-singlet version in which the matrix of Hamiltonian  $\mathcal{H}_0$  in the basis of eigenfunctions of  $\mathcal{H}_{cr}$  is of the form

$$\begin{pmatrix} \mu_1 H_z & 0 & \alpha & \beta \\ 0 & -\mu_1 H_z & \alpha & \pm \beta \\ \alpha & \alpha & \Delta_1 & 0 \\ \beta & \pm \beta & 0 & \Delta_2 \end{pmatrix},$$

i.e., including the case in which both singlets, at distances  $\Delta_1$  and  $\Delta_2$ , are admixed to the ground state. The calculation showed that for any possible values of the parameters  $\alpha$  and  $\beta$  at which the shape of the  $M(H)$  and  $\chi(T)$  curves are in reasonable agreement with experiment, there is practically no anisotropy of the magnetic moment. Since, as we have noted above, the presence of nonequivalent sites makes it so that allowance for the next excited levels ( $\Delta \gtrsim 100$  K) will not give an additional contribution to the anisotropy, it must be concluded that a level system corresponding to the doublet-singlet-singlet version, even in a calculation with all six parameters of Hamiltonian (6), cannot describe the experimentally observed anisotropic behavior of the magnetization of the single crystal.

Thus we can say that the doublet-doublet version is the only possible level system, with the sole proviso that the experimental data presented above for the susceptibility, magnetization, and specific heat can be described not only on the basis of a level system with the ground-state doublet  $a|\pm 5\rangle - b|\mp 1\rangle$  (version I) but can be described equally well when the ground state is the doublet  $a'|\pm 4\rangle - b'|\mp 2\rangle$  (version I'). As is shown below, this ambiguity in the solution can be eliminated by considering the temperature and field dependence of the magnetostriction.

There is every reason to assume that allowance for the two remaining terms in Hamiltonian (6) with  $B_4^3, B_6^3 \neq 0$ , which mix states with  $|\Delta J_z| = 3$ , will lead only to a change in the form of the wave functions for each energy state and will

not substantially alter the arrangement of the energy levels, since in solving the problem we used as parameters the values of the magnetic moments of both doublets and the distance between them, which are rather rigidly fixed by the experimental curves of  $M(H)$  and  $C(T)$  given in Figs. 3 and 4.

## V. MAGNETOSTRICTION OF $Tb_2Ti_2O_7$

Our studies show that a distinctive feature of the energy spectrum of  $Tb^{3+}$  ions in the crystalline field of  $Tb_2Ti_2O_7$  is that, unlike the case in the other  $Ln_2Ti_2O_7$  compounds, there is a nearby doublet which is strongly admixed to the ground-state doublet by the magnetic field. Their components are then a superposition of states  $|J_z\rangle$ , which are also strongly intermixed by the crystalline field. In accordance with the main conclusions of Ref. 3, when the lower energy levels have such a structure the single-ion mechanism involving the interaction of  $4f$  electrons with the crystalline field of the lattice can bring about a significant magnetostriction in the compound under study.

It must be admitted that the theoretical treatment of the magnetostriction properties of both polycrystalline materials and single crystals containing nonequivalent ions in the unit cell runs up against certain difficulties. In particular, the net strain of the unit cell is generally treated as an average over the microstrains due to the nonequivalent ions but is assumed to be uniform over the entire volume of the single crystal.

An analogous model of uniform strain can also be used in calculating the magnetostriction of a polycrystalline sample. In other words, we shall assume that the change in the dimensions of an individual crystallite is similar to the change in the dimensions of the polycrystalline sample as a whole. According to this model, we assume the elastic energy is given by the expression obtained in Ref. 11 for an isotropic solid:

$$U = \frac{1}{2} \sum_{i=1}^6 G_i q_i^2, \quad (13)$$

where  $G_1 = K$  is the bulk modulus,  $G_2 = 3G_3 = G_4/4 = G_5/4 = G_6/4 = \mu_U$  is the shear modulus, and  $q_i$  is expressed in terms of the components of the strain tensor  $\epsilon_{\alpha\beta}$ :

$$\begin{aligned} q_1 &= \epsilon_{xx} + \epsilon_{yy} + \epsilon_{zz}, & q_2 &= \epsilon_{xx} - \epsilon_{yy}, & q_3 &= \epsilon_{xx} + \epsilon_{yy} - 2\epsilon_{zz}, \\ q_4 &= \epsilon_{yz}, & q_5 &= \epsilon_{zx}, & q_6 &= \epsilon_{xy}. \end{aligned} \quad (14)$$

The Hamiltonian of the electron-strain interaction in the variables  $q_i$  is of the form

$$\mathcal{H}' = \sum_s \mathcal{H}'(s), \quad \mathcal{H}'(s) = \sum_{k,m,i} B_{ki}^m(s) O_k^m(s) q_i^{(s)}, \quad (15)$$

where  $s$  labels the magnetic ions in the unit cell, and the operators  $O_k^m(s)$  and the strain variables  $q_i^{(s)}$  are written in the local symmetry axes of ion  $s$ . Following the standard procedure of minimizing the free energy with respect to the components of the strain tensor, we determine  $q_i$  from the condition

$$\text{Sp } \rho \frac{\partial (\mathcal{H}' + \Omega U)}{\partial q_i} = 0. \quad (16)$$

Here

$$\rho = \exp(-\mathcal{H}_0/kT) / \text{Sp} \exp(-\mathcal{H}_0/kT), \quad \mathcal{H}_0 = \sum_s \mathcal{H}_0(s),$$

$\mathcal{H}_0$  is the Hamiltonian of ion  $s$  in the crystalline and magnetic fields, and  $\Omega$  is the volume of the unit cell. We find from (16) that the strain due to the magnetic field is given by

$$\Delta q_i = -\frac{1}{G_i \Omega} \sum_{skmj} B_{skmj}^m(s) [\langle O_k^m(s) \rangle - \langle O_k^m(s) \rangle_0] T_{ji}^{(s)}, \quad (17)$$

where  $\langle O_k^m \rangle = \text{Sp} \rho O_k^m$ ,  $\langle O_k^m \rangle_0$  is the thermal average evaluated for  $H = 0$ , and

$$T_{ji}^{(s)} = \partial q_i^{(s)} / \partial q_j.$$

Let us choose a coordinate system  $x, y, z$  such that the  $z$  axis is directed along  $\mathbf{H}$ . Then the strain tensor  $\varepsilon_{\alpha\beta}$  of the polycrystalline material is diagonal, with  $\varepsilon_{xx} = \varepsilon_{yy}$ . Accordingly, the only nonzero results in (17) are  $\Delta q_1$  and  $\Delta q_3$ . Performing the average over all orientations of the crystallites in the polycrystalline sample and taking into account the local symmetry properties of the crystalline field ( $D_{3d}$ ), we obtain an expression for the isotropic part of the magnetostriction:

$$\left(\frac{\Delta l}{l}\right)_0 = \frac{1}{3} \overline{\Delta q_1} = \sum_{km} A_{k1}^m \int_0^{\pi/2} [\langle O_k^m \rangle - \langle O_k^m \rangle_0] \sin \theta d\theta, \quad (18)$$

and for the components of the anisotropic part:

$$\begin{aligned} \left(\frac{\Delta l}{l}\right)_{\parallel} &= \frac{1}{3} (\overline{\Delta q_1} - \overline{\Delta q_3}) \\ &= \left(\frac{\Delta l}{l}\right)_0 + \sum_{km} A_{k3}^m \int_0^{\pi/2} [\langle O_k^m \rangle - \langle O_k^m \rangle_0] (1 - 3 \cos^2 \theta) \sin \theta d\theta, \\ (\Delta l/l)_{\perp} &= \overline{\Delta q_1} / 3 + \overline{\Delta q_3} / 6, \end{aligned} \quad (19)$$

where

$$A_{k1}^m = -\frac{n}{3K\Omega} B_{k1}^m, \quad A_{k3}^m = -\frac{n}{2\mu_V \Omega} B_{k3}^m \quad (20)$$

and  $n$  is the number of magnetic ions in the unit cell. Because the operators  $O_k^m$  appearing in (18) and (19) should transform according to a unitary representation of the group of the local environment, the only nonzero magnetostriction parameters are  $A_{2i}^0, A_{4i}^0, A_{4i}^3, A_{6i}^0, A_{6i}^3, A_{6i}^6$  ( $i = 1, 3$ ).

The experimental data (Sec. III) imply that the isotropic contribution to the magnetostriction is substantially smaller than  $(\Delta l/l)_{\parallel}$  but nonzero. In order to eliminate this contribution from consideration and thereby to halve the number of parameters in the calculation of the anisotropic magnetostriction, the theoretical temperature and field curves obtained by the formula

$$\begin{aligned} \frac{\Delta l}{l} &= \frac{2}{3} \left[ \left(\frac{\Delta l}{l}\right)_{\parallel} - \left(\frac{\Delta l}{l}\right)_{\perp} \right] \\ &= \sum_{km} A_{k3}^m \int_0^{\pi/2} [\langle O_k^m \rangle - \langle O_k^m \rangle_0] (1 - 3 \cos^2 \theta) \sin \theta d\theta, \end{aligned} \quad (21)$$

were compared to the corresponding experimental curves of

$$(\Delta l/l) = 2[(\Delta l/l)_{\parallel} - (\Delta l/l)_{\perp}] / 3.$$

Our studies have shown that in spite of the large number of experimental curves of  $\Delta l(H, T)/l$ , one cannot by direct comparison with the theoretical curves obtain unambiguous information about the values of the true magnetostriction parameters even if the number of these parameters is limited to four (to the number of parameters of the original static crystalline field). It turns out that, within the accuracy of the model, the same  $\Delta l(H, T)/l$  curves can be described by different sets of parameters  $A_{k3}^m$ .

Nevertheless, the model permits not only a qualitative but also a quantitative description of the field and temperature dependences of the magnetostriction using reasonable values of certain effective parameters. In particular, if we consider only the two lowest doublets of the level system of the  $\text{Tb}^{3+}$  ion and neglect the contribution to the magnetostriction from the higher-lying levels, it becomes possible to replace the entire set of parameters  $A_{k3}^m$  by a single effective parameter  $A_{\text{eff}}$ .

In fact, the specific form of the two lowest doublets in versions I and I' is such that one can obtain an exact (outside of perturbation theory) expression for  $\delta \langle O_k^m \rangle = \langle O_k^m \rangle - \langle O_k^m \rangle_0$

$$\delta \langle O_k^m \rangle = a_k^m f(H, T, \theta), \quad (22)$$

where

$$\begin{aligned} a_k^m &= 1/2 [\langle \psi_3 | O_k^m | \psi_3 \rangle - \langle \psi_1 | O_k^m | \psi_1 \rangle], \\ f(H, T) &= \text{th}(\Delta/2T) - (\rho_1 - \rho_3) \gamma_1 - (\rho_2 - \rho_4) \gamma_2. \end{aligned}$$

Here

$$\psi_1 = \cos \xi_1 |5\rangle + \sin \xi_1 |-1\rangle, \quad \psi_3 = \cos \xi_2 |4\rangle + \sin \xi_2 |-2\rangle,$$

$$\rho_i = \exp(-E_i/T) / \sum_{h=1}^4 \exp(-E_h/T),$$

$$\begin{aligned} E_{1,3} &= 1/2 \{ \Delta - (\mu_1 + \mu_2) H_z \mp [ \Delta + (\mu_1 - \mu_2) H_z ]^2 + V^2 \}^{1/2}, \\ E_{2,4} &= 1/2 \{ \Delta + (\mu_1 + \mu_2) H_z \mp [ \Delta + (\mu_2 - \mu_1) H_z ]^2 + V^2 \}^{1/2}, \\ V^2 &= (H^2 - H_z^2) \mu_{12}, \end{aligned}$$

$$\gamma_1 = [ \Delta + (\mu_1 - \mu_2) H_z ] \{ [ \Delta + (\mu_1 - \mu_2) H_z ]^2 + V^2 \}^{-1/2},$$

$$\gamma_2 = [ \Delta + (\mu_2 - \mu_1) H_z ] \{ [ \Delta + (\mu_2 - \mu_1) H_z ]^2 + V^2 \}^{-1/2},$$

$$\mu_1 = (6 \cos^2 \xi_1 - 1) g_J \mu_B, \quad \mu_2 = (6 \cos^2 \xi_2 - 2) g_J \mu_B,$$

$$\mu_{12} = (\sqrt{22} \cos \xi_1 \cos \xi_2 + \sqrt{40} \sin \xi_1 \sin \xi_2) g_J \mu_B,$$

and  $\mu_1$  and  $\mu_2$  are the magnetic moments of the lower and upper doublet, respectively. Thus the contribution to  $\Delta l/l$  from the two lowest doublets is given by the expression

$$\Delta l/l = A_{\text{eff}} \Phi(H, T), \quad (23)$$

where

$$\Phi(H, T) = \int_0^{\pi/2} f(H, T, \theta) (1 - 3 \cos^2 \theta) \sin \theta d\theta, \quad (24)$$

$$A_{\text{eff}} = \sum_{km} A_{k3}^m a_k^m; \quad (25)$$

$A_{\text{eff}}$  is independent of the temperature and field strength and

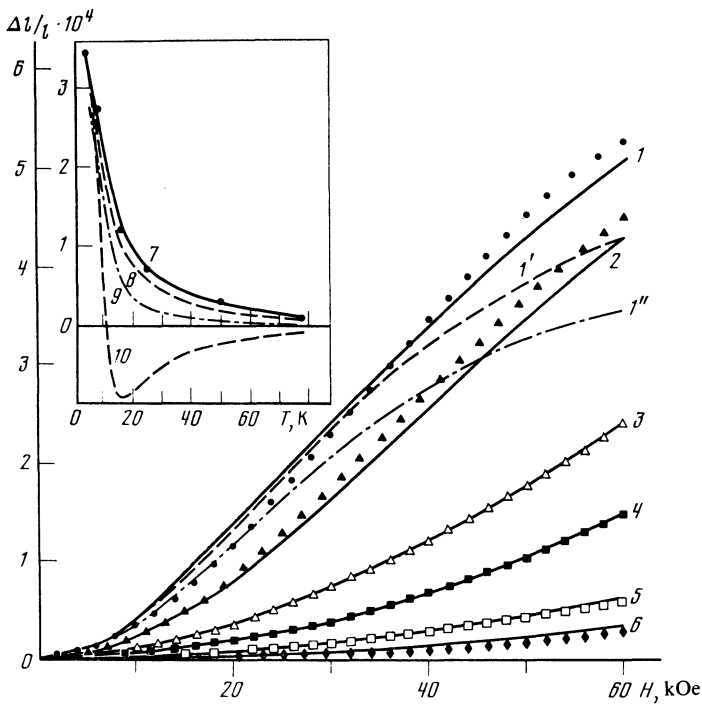


FIG. 6. Magnetic-field dependence of  $\Delta l/l = 2/3[(\Delta l/l)_{\parallel} - (\Delta l/l)_{\perp}]$  in polycrystalline  $\text{Tb}_2\text{Ti}_2\text{O}_7$  at temperatures  $T$  [K]: 1, ●) 4.2; 2, ▲) 8; 3, △) 16; 4, ■) 25; 5, □) 50; 6, ◆) 78. The points are experimental, the solid curves are calculated by Eq. (21), which corresponds to the version-I level system with parameters  $A_{43}^0 = 0.009 \langle J || \beta || J \rangle$  and  $A_{63}^0 = -0.017 \langle J || \gamma || J \rangle$ . 1', 1'') calculation for  $T = 4.2$  K with a single magnetostriction parameter for, respectively, the five lowest energy levels ( $N = 8$ ) and the two lowest doublets ( $N = 4$ ) of version I. The inset shows the temperature dependence of  $\Delta l/l$  at  $H = 40$  kOe: the points are experimental; curves 7 and 8 are calculated for  $N = 8$  in the version-I level system with two parameters and one parameter  $A_{k3}^m \neq 0$ , respectively; curves 9 and 10 are calculated for the two lowest doublets of versions I and I', respectively.

determines only the absolute value of the striction.

The  $\Delta l(H, T)/l$  curves calculated by formula (23) for the two lowest doublets of the version-I level system ( $\mu_1 = 2.35g_J\mu_B$ ,  $\mu_2 = 2g_J\mu_B$ ,  $\mu_{12} = 5.3g_J\mu_B$ ) with  $A_{\text{eff}} = 0.003$  are shown in Fig. 6. The value of the parameter  $A_{\text{eff}}$  was obtained by "tying in" to the point  $T = 4.2$  K and  $H = 10$  kOe. We see that even this two-doublet model (with  $N = 4$  states) gives qualitative agreement with the experimental  $\Delta l(H, T)/l$  curves. With this value of  $A_{\text{eff}}$ , the values of the coefficients  $B_{k3}^m$  calculated by formula (20) differ from the parameters  $B_k^m$  of the static crystalline field (12) by no more than a factor of four, in agreement with the empirical rule  $|B_{ki}^m| \sim |B_k^m|$  established in a study of the spin-lattice relaxation of rare earth ions in crystals.<sup>12</sup> [The values used in formula (20) were  $n = 16$ ,  $\Omega = 10^{-21}$  cm<sup>3</sup>,  $\mu_U = 1.9 \cdot 10^{11}$  erg/cm<sup>3</sup>; an estimate of the shear modulus was obtained from measurements of Young's modulus in polycrystalline  $\text{Tb}_2\text{Ti}_2\text{O}_7$  ( $E = 5.6 \cdot 10^{11}$  erg/cm<sup>3</sup>) under the assumption  $K > \mu_U$ .]

Better agreement of the theoretical and experimental curves can be obtained by taking a large number of energy levels into account and calculating the magnetostriction using two parameter  $A_{\text{eff}}$ . Figure 6 shows for comparison the curves  $\Delta l(H, T)/l$  calculated with allowance for the five lowest levels ( $N = 8$ ) of version I, which are situated below 300 K. It turns out that in this case the entire set of experimental curves can also be satisfactorily described on the basis of a single magnetostriction parameter, for example  $A_{63}^0 = -0.014 \langle J || \gamma || J \rangle = 1.6 \cdot 10^{-8}$  (this value corresponds to  $A_{63}^0 = A_{\text{eff}}/a_6^0$ , where  $A_{\text{eff}} = 0.003$ , with the remaining parameters assumed to be zero).

The solid curves in Fig. 6, which were obtained using formula (21) with two parameters  $A_{63}^0 = -0.017 \langle J || \gamma || J \rangle = 1.1 \cdot 10^{-6}$  ( $N = 8$ ), differ from the experimental curves by no more than 10%. (This fact may

indicate that  $A_{63}^0$  and  $A_{43}^0$  really are the governing terms in the series of true magnetostriction parameters.)

It should be noted that the model used has not only permitted a qualitative and quantitative description of the whole set of existing experimental curves of  $\Delta l/l$  in the temperature range 4.2–80 K at fields up to 60 kOe but has also enabled us, through a comparison of the calculated curves for versions I and I' of the level system, to decide conclusively in favor of the first of these. In fact, one can describe the whole complex of curves on the basis of version I' only by using such large values of the parameters  $A_{23}^0$ ,  $A_{43}^0$ ,  $A_{63}^0$ , and  $A_{63}^6$  that the parameters  $B_{k3}^m$  calculated by (20) differ by two orders of magnitude from the corresponding parameters of the static crystalline field. If we consider a system of two doublets differing from version I in that the lower doublet is  $\psi_{1,2} = 0.846|\pm 4\rangle - 0.532|\mp 2\rangle$ , we find that the field dependence of the magnetostriction in this case is nonmonotonic, exhibiting a maximum at  $H = 30$  kOe. On a change in temperature the magnetostriction of the two-doublet system changes sign, and the overall form of the temperature dependence, shown in the inset in Fig. 6, differs qualitatively from that observed experimentally. Thus our analysis of the magnetostriction properties of a simple two-level system allows us to drop version I' from consideration.

In conclusion, we should point out that expression (23), obtained for  $\Delta l(H, T)/l$  in the particular case of two non-Kramers doublets  $\psi_{1,2}$  and  $\psi_{3,4}$  (see Table I), is also valid in other cases where, in the two-doublet approximation and in the basis of eigenfunctions of  $\mathcal{H}_{\text{cr}}$ , the matrix of Hamiltonian  $\mathcal{H}_0$  decomposes into two blocks and the off-diagonal matrix elements of the operators  $O_k^m$  are equal to zero. This expression, which contains the level separation  $\Delta$  as a parameter, makes it possible to study rather simply the dependence of the magnetostriction on the value of this parameter. For example, by leaving all the parameters except  $\Delta$

unchanged, we find that as  $\Delta$  changes from 16 to 160 K the value of the magnetostriction falls by two orders of magnitude.

It follows from the form of formulas (18) and (19) that the magnetostriction caused by the single-ion mechanism is in general determined not only by the structure of the energy levels, which is built into the difference of the thermal averages [ $\langle O_k^m \rangle - \langle O_k^m \rangle_0$ ], but also by the elastic constants and the electron–lattice interaction parameters. The present study, together with the study of the magnetostriction in other members of the homologous series  $\text{Ln}_2\text{Ti}_2\text{O}_7$ , allows us to rule out the last two factors, which do not change substantially within the homologous series, and to reveal the influence of the first in pure form. It turns out that the presence of a nearby excited state which is strongly intermixed with the ground state by a magnetic field is sufficient to cause the magnetostriction typical of other investigated compounds of the  $\text{Ln}_2\text{Ti}_2\text{O}_7$  series (which have  $\Delta > 100 \text{ K}$ )<sup>5</sup> to increase to the giant proportions in  $\text{Tb}_2\text{Ti}_2\text{O}_7$ .

We are grateful to A. V. Kolesnikov for growing the single crystal and to V. I. Sokolov, Z. A. Kazeĭ, and A. S. Markosyan for the opportunity to use the vibration magnetometer and Geigerflex diffractometer and for assistance in the measurements on this equipment.

<sup>1)</sup> Imperfection of a structure of the pyrochlore type can be due, for example, to the possibility of intersubstitution of the ions  $\text{Ti}^{4+}$  and  $\text{Ln}^{3+}$ .

<sup>1)</sup> K. P. Belov, G. I. Kataev, R. Z. Levitin, S. A. Nikitin, and V. I. Sokolov, *Usp. Fiz. Nauk* **140**, 271 (1983) [*Sov. Phys. Usp.* **26**, 518 (1983)].

<sup>2)</sup> L. A. Bumagina, V. I. Krotov, B. Z. Malkin, and A. Kh. Khasanov, *Zh. Eksp. Teor. Fiz.* **80**, 1543 (1981) [*Sov. Phys. JETP* **53**, 792 (1981)].

<sup>3)</sup> I. V. Aleksandrov, L. G. Mamsurova, K. K. Pukhov, N. G. Trusevich, and L. G. Shcherbakova, *Pis'ma Zh. Eksp. Teor. Fiz.* **34**, 68 (1981) [*JETP Lett.* **34**, 63 (1981)].

<sup>4)</sup> G. A. Babushkin, A. K. Zvezdin, R. Z. Levitin, V. N. Orlov, and A. I. Popov, *Zh. Eksp. Teor. Fiz.* **85**, 1366 (1983) [*Sov. Phys. JETP* **58**, 792 (1983)].

<sup>5)</sup> L. G. Mamsurova, K. K. Pukhov, N. G. Trusevich, and L. G. Shcherbakova, *Fiz. Tverd. Tela (Leningrad)* **27**, 2023 (1985) [*Sov. Phys. Solid State* **27**, 1214 (1985)].

<sup>6)</sup> S. A. Al'tshuler and B. M. Kozyrev, *Elektronnyĭ Paramagnitnyĭ Rezonans (Electron Paramagnetic Resonance)*, Nauka, Moscow (1972), p. 106.

<sup>7)</sup> L. G. Shcherbakova, L. G. Mamsurova, and G. E. Sukhanova, *Usp. Khim.* **48**, 423 (1979).

<sup>8)</sup> V. I. Sokolov, *Prib. Tekh. Eksp.*, No. 5, 206 (1971).

<sup>9)</sup> A. Abragam and B. Bleaney, *Electron Paramagnetic Resonance of Transition Ions*, Clarendon Press, Oxford (1970).

<sup>10)</sup> C. L. Chien and A. W. Sleight, *Phys. Rev. B* **18**, 2031 (1978).

<sup>11)</sup> L. D. Landau and E. M. Lifshitz, *Theory of Elasticity*, 2nd ed., Pergamon Press, Oxford 1970 [p. 202 in Russian original].

<sup>12)</sup> C. D. Jeffries, *Dynamic Nuclear Orientation*, Interscience, New York (1963) [p. 56 in Russian translation].

Translated by Steve Torstveit